CHALMERS
UNIVERSITY OF TECHNOLOGY

FPGA-based Optical Kerr Effect Emulator

FPGA-based Optical Kerr Effect Emulator

Keren Liu[1], Erik Börjeson[1], Christian Häger[2], and Per Larsson-Edefors[1]

[1]*Dept. of Computer Science and Engineering, Chalmers University of Technology, Gothenburg, Sweden*
[2]*Dept. of Electrical Engineering, Chalmers University of Technology, Gothenburg, Sweden*
perla@chalmers.se

Abstract: We propose a digital emulator of the optical Kerr effect, suitable for FPGA implementation. In addition, we study a combined PMD and Kerr emulator implementation with respect to DSP hardware aspects such as fixed-point performance.

1. Introduction

In fiber-optic communication, there are several impairments that affect the BER performance at the receiver. The linear polarization-mode dispersion (PMD) and the nonlinear optical Kerr effect have a combined detrimental effect on the transmitted signal [1], but this effect can be complex to study as PMD varies over time. To thoroughly assess the impact of the combined PMD-Kerr effect on a receiver DSP implementation, one option is to conduct optical transmission experiments. However, besides requiring expensive equipment, experimental setups can be challenging to integrate with real-time DSP and often lack precise control of the underlying channel parameters.

The Fiber-on-Chip approach [2] offers an alternate way to perform real-time analysis of a fiber-optic communication system. Here, a *digital system model* runs in real-time on an FPGA, making real-time control and analysis straightforward. This paper extends our previous work in [2, 3] and proposes a digital emulator of the optical Kerr effect that, in combination with the PMD emulator in [3], forms a real-time PMD-Kerr emulator that is suitable for implementation on an FPGA.

2. Digital Emulation of Optical Kerr Effect

Our digital Kerr effect emulator is based on a numerical solution to the Manakov-PMD equation [4], in which a fiber is divided into multiple PMD sections. Each section's Kerr effect is modeled as $\hat{\boldsymbol{u}} = \boldsymbol{u}\exp(j\bar{\gamma}\|\boldsymbol{u}\|^2)$, where $\boldsymbol{u} = [u_x(t,z), u_y(t,z)]^\top$ is the Jones vector of the complex baseband signals in the x and y polarizations, t and z are the propagation time and distance, respectively, and $\bar{\gamma} = \frac{8}{9}\gamma L$ represents the Kerr parameter γ multiplied by the section length L and the averaging coefficient $\frac{8}{9}$. This model can be further written as

$$\begin{cases} \hat{u}_{xi} = u_{xi}\cos(\phi) - u_{xq}\sin(\phi) \\ \hat{u}_{xq} = u_{xi}\sin(\phi) + u_{xq}\cos(\phi) \end{cases}, \quad \begin{cases} \hat{u}_{yi} = u_{yi}\cos(\phi) - u_{yq}\sin(\phi) \\ \hat{u}_{yq} = u_{yi}\sin(\phi) + u_{yq}\cos(\phi) \end{cases}, \quad \phi = \bar{\gamma}(u_{xi}^2 + u_{xq}^2 + u_{yi}^2 + u_{yq}^2), \tag{1}$$

where $u_x = u_{xi} + ju_{xq}$ and $u_y = u_{yi} + ju_{yq}$ are the inputs and $\hat{\square}$ denotes the outputs.

Fig. 1 shows a block diagram of the digital Kerr effect emulator, which is pipelined to balance the timing paths and increase the clock speed. A look-up table (LUT), which comprises all sine values, is indexed by the input angle ϕ with a range of $[0, \pi/2]$. The Limit block converts the angle to the range $[0, \pi/2]$.

3. Emulator Structure

The combined PMD-Kerr emulator developed in this paper uses a transmitter from the CHOICE environment [5,6] and PMD emulator components developed in [3]. Fig. 2 illustrates the system structure, inside which emulation of the combined impacts of PMD and the Kerr effect is realized. The pseudo-random data sequence used for transmission over two polarizations is modulated to QPSK before being upsampled to two samples per symbol and convolved with a 51-tap root-raised-cosine (RRC) filter with a roll-off factor of 0.1.

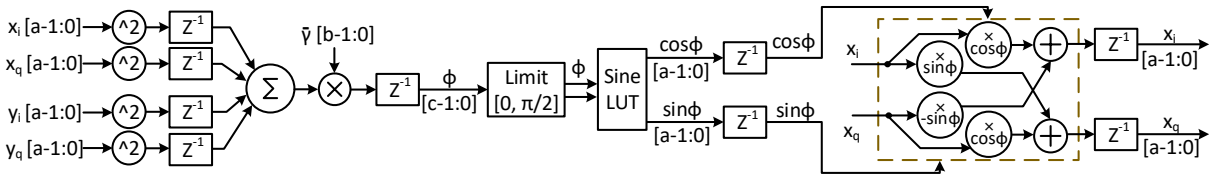

Fig. 1: Block diagram of the Kerr effect emulator. Registers are represented by z^{-1}. The boxed rotation block is shown only for the x polarization, and the rotation block for the y polarization is a duplication of the shown one. The inputs to the rotation block are also delayed by three z^{-1} which are not shown.

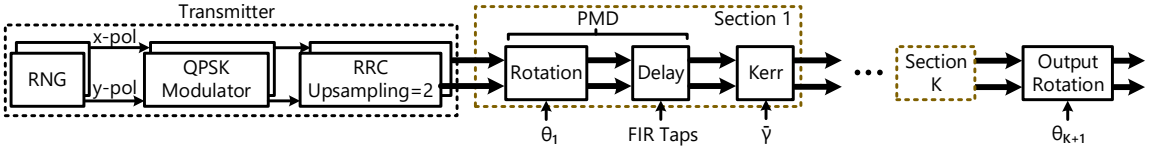

Fig. 2: Block diagram of the proposed PMD-Kerr emulation system.

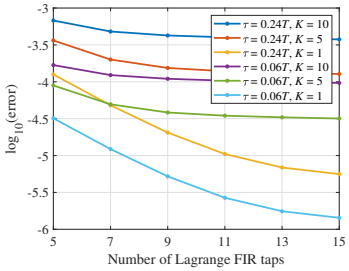

Fig. 3: Performance of TD MATLAB vs FD MATLAB (x-pol).

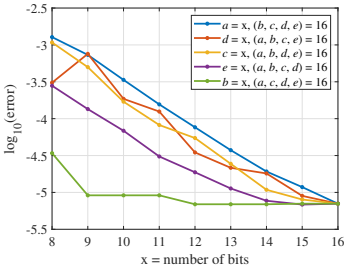

Fig. 4: Performance of digital emulator vs TD MATLAB reference (x-pol).

	Type	$K=1$	$K=10$
Kerr	LUT	2,283 (0.53%)	21,285 (4.91%)
	DSP	26 (0.72%)	260 (7.22%)
Total	LUT	8,415 (1.94%)	27,910 (6.44%)
	DSP	170 (4.72%)	944 (26.22%)

Table 1: Resource utilization on Xilinx VC709. The *Kerr* entry includes all Kerr modules in the system. The values are given as *number of used blocks (ratio of used blocks to available blocks)*.

The digital PMD model consists of multiple concatenated sections [3] and the Kerr emulator is inserted in each section after the PMD emulator. Each PMD section contains one Rotation and one Delay component. The former rotates the x and y polarization with an angle of θ_k in section k, while the latter utilizes an n-tap Lagrange fractional-delay filter (similar to [7]) to apply a differential group delay (DGD) of τ between the two polarizations. Here, τ is a fraction of the symbol period (T). The rotation angle θ_k can be time varying and different for each section, while the DGD τ and the Kerr parameter $\bar{\gamma}$ are kept the same in all sections for simplicity.

4. Analysis of Performance and Resource Utilization

We first perform floating-point MATLAB simulations to compare the time-domain (TD) PMD-Kerr model, which uses an n-tap Lagrange filter to realize DGD, with a reference frequency-domain (FD) PMD-Kerr model, which uses a DGD based on FFT/IFFT. The system assumptions are $\bar{\gamma} = \frac{1120}{9}$ rad/W (assuming $\gamma = 1.4$ rad/W/km and $L = 100$ km) and an overall transmitted power of 0 dBm. The θ_k, $k = 1,2,...,K+1$ is randomly generated with a uniform distribution on $[-\pi,\pi]$ and is kept unchanged during the simulations. Fig. 3 shows the results for a 16,384-sample simulation, where n is varied from 5 to 15, while $\tau \in \{0.06T, 0.24T\}$ and $K \in \{1,5,10\}$. The error is calculated as $\overline{|(x_i^0 - x_i^1) + j(x_q^0 - x_q^1)|}$ or $\overline{|(y_i^0 - y_i^1) + j(y_q^0 - y_q^1)|}$, in which 0 and 1 denote the two models.

To further evaluate our proposed emulator, we use logic simulations to compare the fixed-point implementation against a TD MATLAB implementation, with $\bar{\gamma} = \frac{1120}{9}$ rad/W, an overall transmitted power of 0 dBm, $\tau = 0.06T$, $K = 10$ and a 5-tap Lagrange filter. The wordlengths a, b, c, d and e are individually varied from 8 to 16: a corresponds to the data sample x_i, x_q, y_i and y_q, b to the Kerr parameter $\bar{\gamma}$, c to the rotation angle θ_k and the Kerr angle ϕ, d to the FIR taps of the Lagrange filter, and e to the RRC taps. All parameters are represented in signed fixed-point format. To average the rounding error caused by the different values of θ_k, for each symbol in the simulation, i.e., two samples, a new set of θ_k, $k = 1,2,...,K+1$ is randomly generated with a uniform distribution on $[-\pi,\pi]$. Fig. 4 shows the results for a simulation with 16,384 samples.

To analyze the resource utilization, we synthesized the system in Fig. 2 to a Xilinx VC709 development board with a 100 MHz clock. We choose 12-bit wordlengths for all signals and use section counts K between 1 and 10. As can be expected, the usage of LUT and DSP resources grows linearly with an increasing K. As Table 1 shows for $K = 10$, the DSP slices are the bottleneck and this 10-section system utilizes 26% of the available DSPs, which leaves enough room for implementing an equalizer on the same FPGA.

Acknowledgements: The work of C. Häger was supported by the Swedish Research Council under grant no. 2020-04718.

References

1. C. R. Menyuk and B. S. Marks, "Interaction of polarization mode dispersion and nonlinearity in optical fiber transmission systems," J. Light. Technol. **24**, 2806 (2006).
2. P. Larsson-Edefors and E. Börjeson, "Fiber-on-Chip: Digital FPGA emulation of channel impairments for real-time evaluation of DSP," in *Opt. Fiber Commun. Conf. (OFC),* (2022), p. W3H.3.
3. H. Kan, H. Zhou, E. Börjeson, M. Karlsson, and P. Larsson-Edefors, "Digital emulation of time-varying PMD for real-time DSP evaluations," in *Asia Communications and Photonics Conference,* (2021), pp. M4H–4.
4. R. Hardin, "Applications of the split-step Fourier method to the numerical solution of nonlinear and variable coefficient wave equations," SIAM Rev. (Chronicles) **15** (1973).
5. E. Börjeson, C. Fougstedt, and P. Larsson-Edefors, "Towards FPGA emulation of fiber-optic channels for deep-BER evaluation of DSP implementations," in *Signal Processing in Photonic Communications,* (2019), pp. SpTh1E–4.
6. CHOICE - Chalmers Optical Fiber Channel Emulator (2022). www.cse.chalmers.se/research/group/vlsi/choice.
7. R. M. Bütler, C. Häger, H. D. Pfister, G. Liga, and A. Alvarado, "Model-based machine learning for joint digital backpropagation and PMD compensation," J. Light. Technol. **39**, 949–959 (2021).